Supplementary Information

Nonaqueous synthesis of metal cyanamide semiconductor nanocrystals for photocatalytic water oxidation

Wei Zhao,[a] Jie Pan[a, b] and Fuqiang Huang[*a, c]

[a] State Key Laboratory of High Performance Ceramics and Superfine Microstructure, Shanghai Institute of Ceramics, Chinese Academy of Sciences, Shanghai 200050, P. R. China

[b] University of Chinese Academy of Sciences, Beijing 100049, China.

[c] State Key Laboratory of Rare Earth Materials Chemistry and Applications, College of Chemistry and Molecular Engineering, Peking University, Beijing 100871, P.R. China

*** E-mail: huangfq@mail.sic.ac.cn (FQH).**

Experimental Section

Nanocrystal growth. All the materials were used as received without further purification. Metal cyanamide nanocrystals including Ag_2NCN nanorods (NRs), ZnNCN NRs and PbNCN nanoparticles (NPs) were synthesized in nonaqueous solution at room temperature. Typically, 1 mmol of metal salt source ($AgNO_3$, $ZnCl_2$ and $PbCl_2$) was dissolved in a mixture solution of 3 mL of toluene and 1 mL of oleylamine (OMA). After stirring for 30 min, 1 mL of 1M cyanamide (H_2NCN) ethanol solution was injected rapidly to proceed the precipitation reaction. After growth for 60 min, 3 ml of acetone was added to stop the reaction, followed by centrifugation and purification for three times with acetone as antisolvent and toluene as solvent. The obtained powder was dried in vacuum oven at room temperature for 6 h. In this protocol, the dissolution of $ZnCl_2$ and $PbCl_2$ was assisted by ultrasonication for about 15 min. The OMA capping agents could be replaced by other primary amines, such as hexadecanylamine (HDA) and octadecanamine (ODA).

Synthesis of Ag_2NCN microcrystals (MCs). Typically, 1 mL of 1M H_2NCN aqueous solution was added rapidly to 5 mL of water containing 1mmol of $AgNO_3$ and 0.2 mL of concentrated NH_4OH (30 vol.%) room temperature under stirring. After stirring for

60 min, the resulting yellow suspension was filtrated, washed with distilled water for three times and then dried at 60 °C in vacuum oven for 6 h.

Ligand exchange of OMA-derived Ag_2NCN NRs. The as-prepared Ag_2NCN NRs were subjected to dilute NH_4OH solution to exchange OMA with OH^-. A stock solution was prepared by dissolving 1 mL of concentrated NH_4OH (30 vol.%) in a mixture containing 25 ml of ethanol and 25 ml of toluene. To conduct ligand exchange, 1 mmol of as-prepared NRs was dispersed in 50 ml of toluene, followed by adding the stock solution under stirring. After exchange for 60 min, the resulting product was washed three times by dispersion in ethanol and precipitation by addition of toluene. Then the obtained powder was dispersed in ethanol and dried in vacuum oven at room temperature for 6 h.

Characterization. Phase analysis was conducted by X-ray diffraction (XRD) using a Bruker D8 ADVANCE diffractometer with Cu-K (1.5406 Å) irradiation. Sample morphology was examined using field emission scanning electron microscope (FESEM, JEOL JSM-6400F) and transmission electron microscope (TEM, JEM2100F). UV-Vis diffuse reflectance spectra were measured at room temperature on a spectrophotometer (Hitachi U3010) in the range from 300 nm to 1500 nm. The Brunauer-Emmett-Teller (BET) specific surface areas were determined through nitrogen sorption isotherms at 77K using a Micromeritics ASAP-2010 instrument and calculated from the linear part of the BET plot. The FTIR measurements were carried out in a Shimadzu FTIR Prestige-21.

Photocatalytic water splitting for oxygen evolution. The photocatalytic oxygen production was carried out in a top-irradiation Pyrex reactor. Ag_2NCN NRs (300 mg) were dispersed in 200 mL of aqueous solution with 0.8 g of $AgNO_3$ as the sacrificial agent. Then the mixture was pursed by pure N_2 for 30 min and illuminated by a 500 W Xe lamp with a cutoff filter ($\lambda \geq 420$ nm). During the test, 0.2 mL of gas evolution was sampled every hour and analyzed using a gas chromatographer (Shanghai, GC-7900,

TCD, N_2 carrier) to measure the O_2 evolution amount. For comparison, Ag_2NCN MCs was used as a reference.

Photocatalytic dye degradation. Methylene blue (MB) was used as a representative organic dye to evaluate the photocatalytic activity of Ag_2NCN NRs under visible-light illumination ($\lambda \geq 420$ nm). 0.1 g of Ag2NCN NRs were dispersed in 100 mL aqueous solution of 10 mg / L MB for photocatalytic evaluation. Visible-light irradiation was conducted after the suspension was magnetically stirred in the dark for 30 min to reach adsorption–desorption equilibrium. During irradiation, about 5 mL of suspension was taken from the mixture at a given time interval and centrifuged; the supernatant was used for MB concentration analysis by a UV-Vis spectrometer. For comparison, commercial P25 powder and Ag_2NCN MCs were selected as reference.

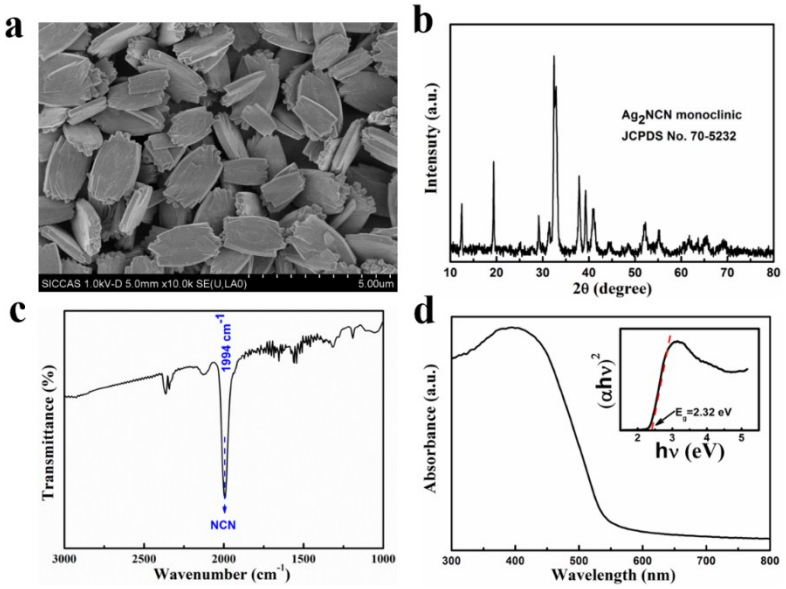

Figure S1. (a) FESEM image, (b) XRD pattern, (c) FTIR spectrum and (d) absorption spectrum of the Ag_2NCN MCs synthesized in aqueous solution.

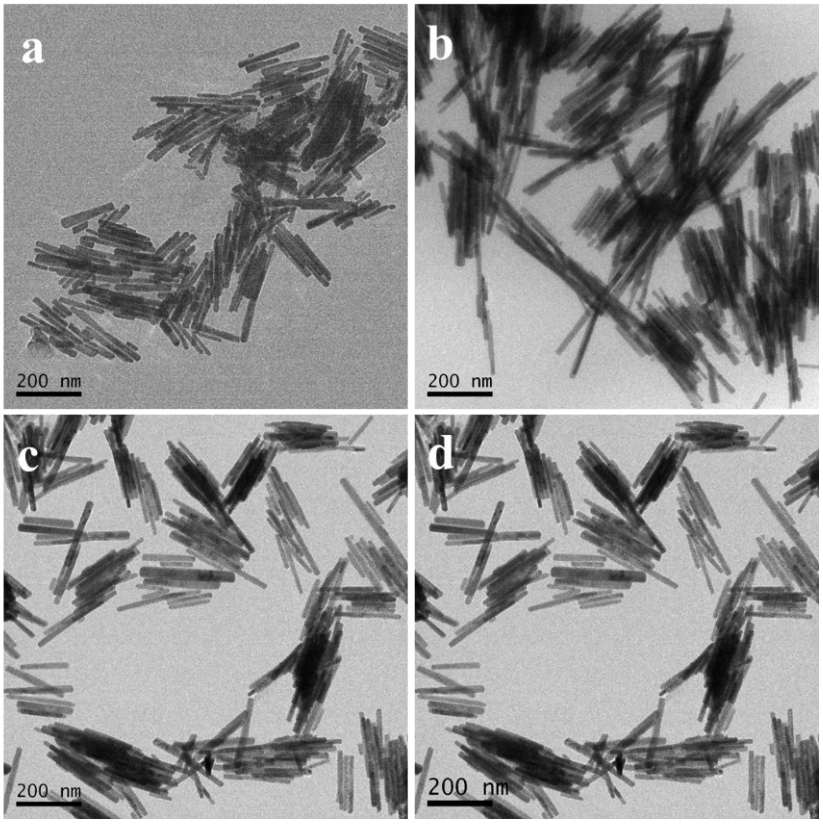

Figure S2. The TEM images of the as-prepared Ag_2NCN NRs along with the reaction time at (a) 1min, (b) 5min, (c) 10 min, and (d) 30 min.

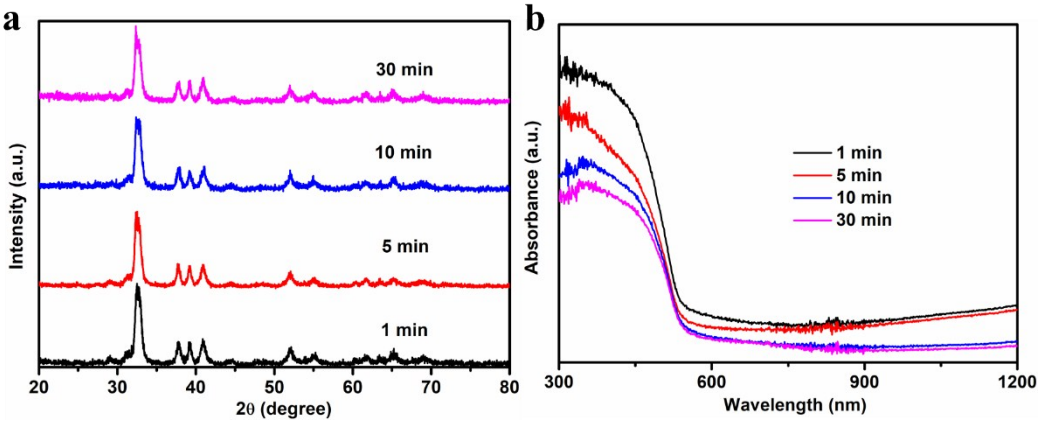

Figure S3. The evolution of the XRD patterns (a) and absorption spectra (b) along with the reaction time.

The formation mechanism of Ag_2NCN NRs is clarified by conducting controlled experiments. The phase and morphology evolution of the samples along with the reaction time are characterized by XRD and TEM, accompanied by monitoring the change of absorption spectra. As shown in Figure S2, rod-like particles with a broad size distribution appeared at the earlier stage of the reaction after injection of H_2NCN to silver salt dissolved solution (1 min). Then the nanoparticles became uniform in size and morphology after further growth (5 min and 10 min) due to size focusing process, which suggested a diffusion-controlled growth mechanism. After 30 min, the size distribution didn't change significantly. Such a similar growth process can be also found in the preparation of copper(I) sulfide NRs. (M. Kruszynska, et. al, ACS Nano, 2012, 6, 5889-5896). The phase evolution indicated the formation of Ag_2NCN NRs in the first 1 min observed from the XRD patterns (Figure S3a). During further growth (5-30 min), the intensity of prominent XRD peaks between 30°-35° increased, indicating a slight enhancement of the crystallinity. The optical property measurement (Figure S3b) showed the characteristic absorption edge of Ag_2NCN after 1 min, consistent with the XRD analysis. With the increase of growth time (5 min), a slight blue-shift could be observed, maybe due to the size effect. During further growth (10-30 min), no obvious change of absorption edge happened. Combining TEM, XRD and Abs measurements, it can be seen that the growth of Ag_2NCN NRs nearly finished in 10 min and obeyed the diffusion-controlled growth mechanism.

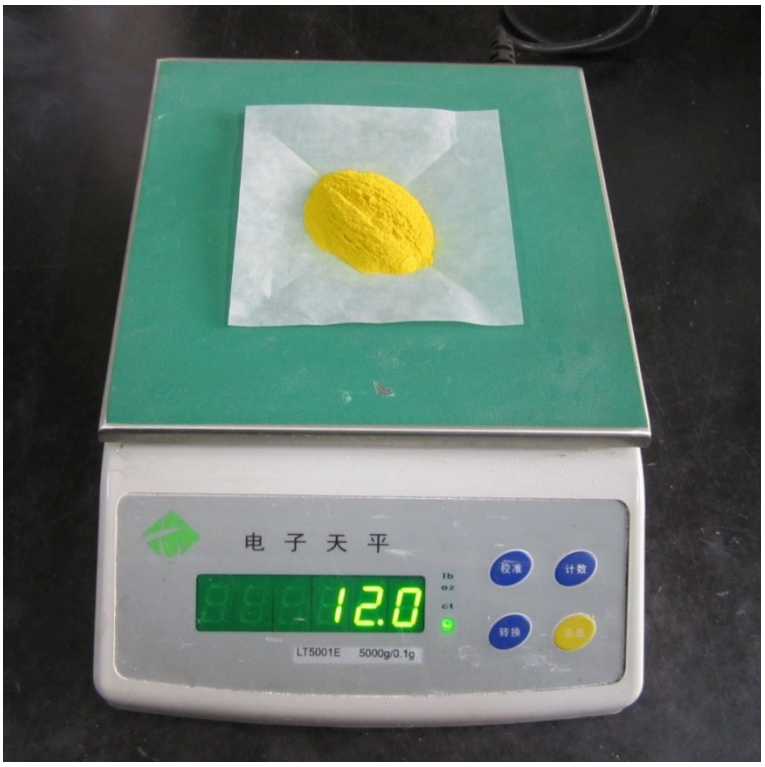

Figure S4. Gram-scale synthesis of Ag_2NCN NRs in one batch.

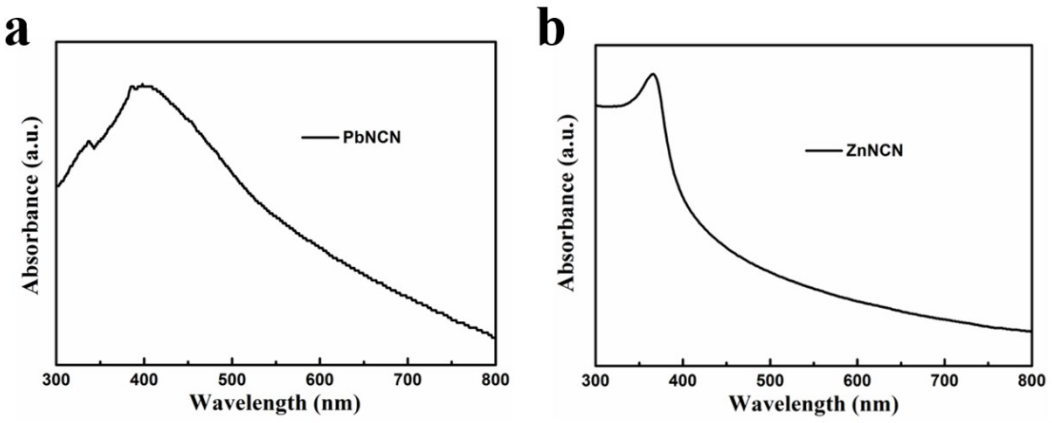

Figure S5. Absorption spectra of the as-prepared ZnNCN NRs and PbNCN NPs.

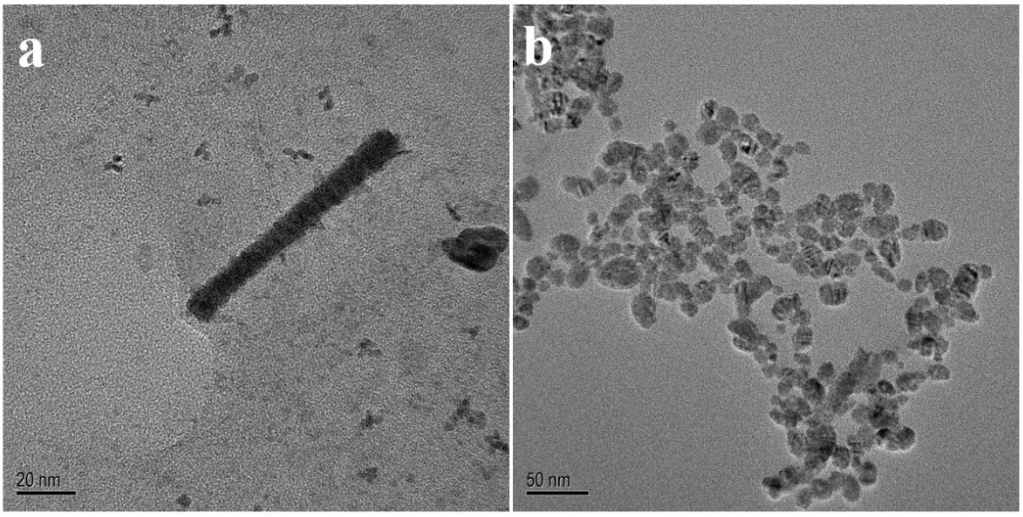

Figure S6. Low-resolution TEM images of the as-prepared (a) ZnNCN NRs and (b) PbNCN NPs.

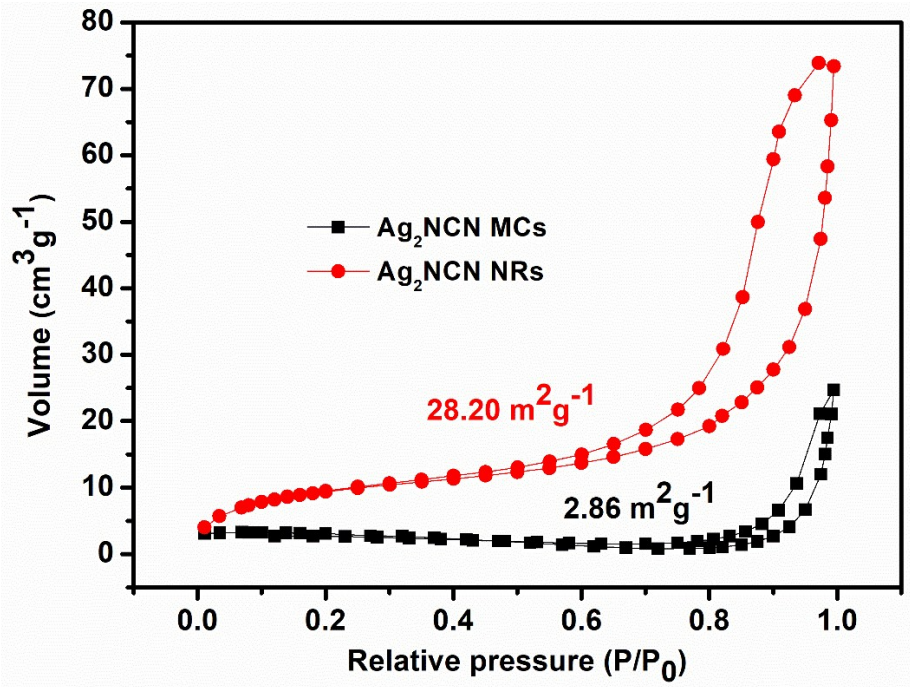

Figure S7. N_2 adsorption-desorption isotherm of Ag_2NCN NRs and MCs.

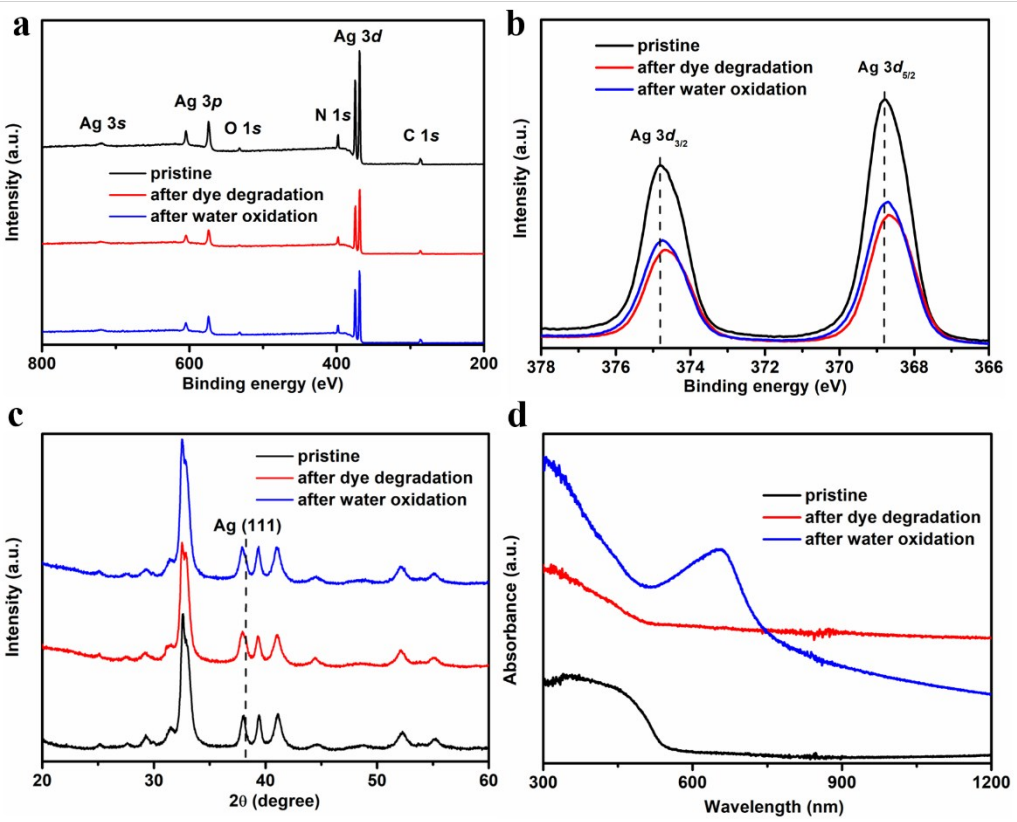

Figure S8. XPS spectra (a, b), XRD patterns (c) and absorption spectra (d) of the Ag_2NCN NRs before and after photocatalytic test.

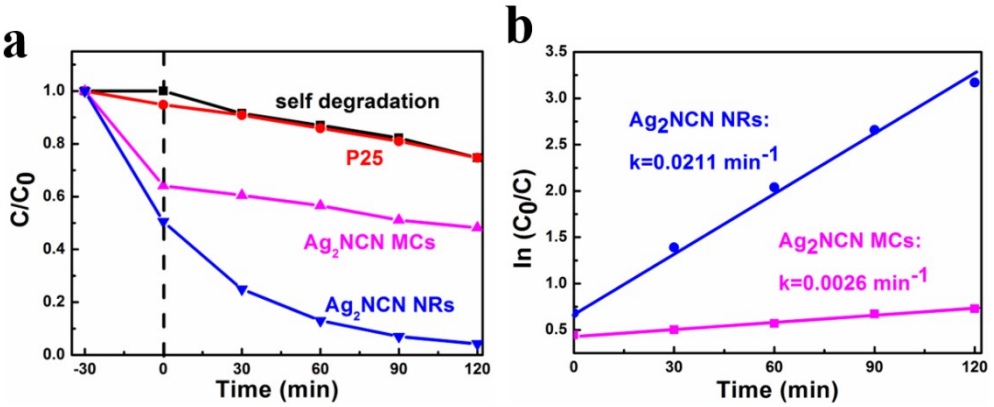

Figure S9. (a) Methylene blue (MB) visible-light ($\lambda \geq 420$ nm) photodegradation tests of Ag_2NCN NRs, MCs and P25. (b) Kinetics analysis of the MB photocatalytic degradation.

The photocatalytic performance of Ag_2NCN NRs towards organic dye degradation (MB, MO, and RhB) under visible-light irradiation is studied with the commercially purchased P25-TiO_2 powder and Ag_2NCN MCs as reference.

As shown in Figure S9a, the Ag_2NCN NRs display higher photocatalytic activity than that of the two reference samples and bleach MB within 120 min, while only 30 % of MB is degraded over Ag_2NCN MCs. Figure S9b depicts the quantitative analysis on the reaction kinetics of MB degradation in the test based on the "pseudo-first order model, expressed as follows: $\ln(C_0 / C) = K t$, where, C_0 and C are the dye concentration at time 0 and t, respectively. *K* is the pseudo-first order reaction rate constant. Clearly, *K* for Ag_2NCN NRs (0.0211 min^{-1}) is much higher than that of Ag_2NCN MCs (0.0026 min^{-1}), demonstrating the superior photocatalytic activity of Ag_2NCN NRs. Besides MB degradation, The Ag_2NCN NRs also show high performance toward the other two type of organic dye degradation, decomposing MO within 90 min and RhB within 60 min (Figure S10).

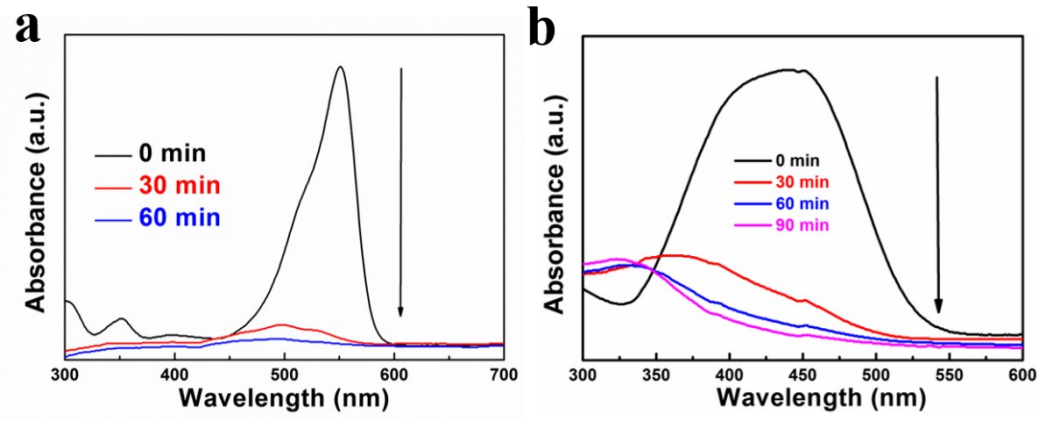

Figure S10. Photocatalytic degradation of (a) RhB and (b) MO under visible-light irradiation. RhB : Rhodamine B; MO : Methyl orange.

Table S1. Oxygen evolution performance of the as-prepared Ag_2NCN NRs compared with some of the typical semiconductors.

Photocatalysts	Specific surface area (m^2g^{-1})	O_2 evolution ($\mu mol\ h^{-1}g^{-1}$)	Test condition	Light source	Ref.
Ag_3PO_4	0.98	1272	0.5 g of photocatalysts, 850 mg $AgNO_3$, 270 mL water	300 W Xeon lamp, $\lambda > 420$ nm	1
$BiVO_4$	1.2	492			
WO_3	-	144			
Mesoporous Bi_2WO_6	15.26	84.8	0.1 g of photocatalysts, 0.1 M $AgNO_3$, 100 mL water	300 W Xeon lamp, $\lambda > 400$ nm	2
Molecular Cobalt modified C_3N_4	-	260	0.05 g of photocatalysts, 0.2 g La_2O_3, 0.01 M $AgNO_3$, 100 mL water	300 W Xeon lamp	3
$Co(OH)_2$ deposited C_3N_4	61	142	0.05 g of photocatalysts, 0.2 g La_2O_3, 0.01 M $AgNO_3$, 100 mL water	300 W Xeon lamp, $\lambda > 420$ nm	4
Mo doped Bi_2WO_6	12.89	147.2	0.1 g of photocatalysts, 0.1 M NaOH, 0.02 M $Na_2S_2O_8$, 100 mL water	300 W Xeon lamp, $\lambda > 420$ nm	5
$BiVO_4$	-	328	0.02 g of photocatalysts, 0.05 M $AgNO_3$, 12 mL water	300 W Xeon lamp, $\lambda > 420$ nm	6
Mo doped $BiVO_4$	-	942	0.01 g of photocatalysts, 0.05 M $AgNO_3$, 11 mL water	plasma lamp, AM 1.5G	7
monoclinic WO_3	4.7	84.7	0.1 g of photocatalysts, 50 mg $AgNO_3$, 100 mL water	300 W Xeon lamp, $\lambda > 420$ nm	8
Ag_2NCN NRs	28.20	280.7	0.3 g of photocatalysts, 80 mg $AgNO_3$, 200 mL water	500 W Xeon lamp, $\lambda > 420$ nm	This work

Reference

S1. Z. Yi, J. Ye, N. Kikugawa, T. Kako, S. Ouyang, H. Stuart-Williams, H. Yang, J. Cao, W. Luo, Z. Li, Y. Liu and R. L. Withers, *Nature Materials*, 2010, **9**, 559-564.

S2. C. Li, G. Chen, J. Sun, J. Rao, Z. Han, Y. Hu and Y. Zhou, *ACS Applied Materials & Interfaces*, 2015, **7**, 25716-25724.

S3. G. Zhang, C. Huang and X. Wang, *Small*, 2015, **11**, 1215-1221.
S4. G. Zhang, S. Zang and X. Wang, *ACS Catalysis*, 2015, **5**, 941-947.
S5. A. Etogo, R. Liu, J. Ren, L. Qi, C. Zheng, J. Ning, Y. Zhong and Y. Hu, *J Materials Chemistry A*, 2016, **4**, 13242-13250.
S6. H. J. Kong, D. H. Won, J. Kim and S. I. Woo, *Chemistry Materials*, 2016, **28**, 1318-1324.
S7. S. M. Thalluri, S. Hernández, S. Bensaid, G. Saracco and N. Russo, *Applied Catalysis B: Environmental*, 2016, **180**, 630-636.
S8. N. Zhang, C. Chen, Z. Mei, X. Liu, X. Qu, Y. Li, S. Li, W. Qi, Y. Zhang, J. Ye, V. A. L. Roy and R. Ma, *ACS Applied Materials & Interfaces*, 2016, **8**, 10367-10374.